

## A new $(C_2H_5NH_3)_2ZnCl_4$ crystal with a pure $Pnma-P2_12_12_1$ ferroelastic phase transition

This article has been downloaded from IOPscience. Please scroll down to see the full text article.

1994 J. Phys.: Condens. Matter 6 6751

(<http://iopscience.iop.org/0953-8984/6/34/007>)

View [the table of contents for this issue](#), or go to the [journal homepage](#) for more

Download details:

IP Address: 171.66.16.151

The article was downloaded on 12/05/2010 at 20:21

Please note that [terms and conditions apply](#).

## A new $(C_2H_5NH_3)_2ZnCl_4$ crystal with a pure $Pnma-P2_12_12_1$ ferroelastic phase transition

M J Tello†, A López-Echarri†, J Zubillaga†, I Ruiz-Larrea†, F J Zúñiga†, G Madariaga† and A Gómez-Cuevas†

† Departamento de Física de la Materia Condensada, Facultad de Ciencias, Universidad del País Vasco, Apartado 644, Bilbao 48080, Spain

‡ Departamento de Física Aplicada II, Facultad de Ciencias, Universidad del País Vasco, Apartado 644, Bilbao 48080, Spain

Received 9 February 1994, in final form 1 June 1994

**Abstract.** Optical, calorimetric, and x-ray measurements performed on  $(C_2H_5NH_3)_2ZnCl_4$  ( $C_2ZnCl$ ) together with a group theoretical analysis have revealed that this crystal shows a pure first-order ferroelastoelectric phase transition at 243.3 K. In the low-temperature phase the crystal shows two explicit forms of ferroicity: gyrotropy and piezoelectricity, which is a common fact in this class of secondary ferroics. The experimental data show that the corresponding phase transition is similar to that observed in  $(C_5H_{11}NH_3)_2ZnCl_4$  ( $C_5ZnCl$ ) at 249 K. The thermodynamic function values for this phase transition in both compounds and the x-ray results confirm that the conformational changes must be excluded from the physical mechanisms involved in the onset of the ferroelastoelectric properties. The microscopic origin of this phase transition should be related to the freezing of the dynamical disorder of the N–H...Cl hydrogen bonding and with the corresponding tilting of the hydrocarbon chains. The experimental data seem to be in agreement with the Landau phenomenological theory except near  $T_c$ , where the experimental specific heat is well described by an empirical power law. Finally, as found in some other crystals of this family,  $C_nZnCl$  crystals also exhibit an isotropic point around 25 K. The isotropic point temperature shows a very strong dependence on  $n$  (chain length) for  $n \leq 5$  and an asymptotic behaviour for  $n \geq 12$ .

### 1. Introduction

Among the structural phase transitions (SPTs), intensive attention has been paid to those crystals that exhibit ferroelectricity or ferroelasticity in the low-temperature phase (distorted phase). However, from a theoretical point of view (group theory) other SPTs exist with a change of point symmetry where the spontaneous quantities, forbidden in the prototype phase, are other than the polarization or the strain. Among these, the so called gyrotropic phase transitions (GPTs), which involve the onset of optical activity, show special interest. The spontaneous order parameter (OP) of these transformations is described by a component (or a combination) of a third-rank tensor [1] called the gyrotropic tensor, which antisymmetric in the first two indices, and which acquires new non-zero components in the distorted phase.

In the last decade, the study of optical activity as a secondary effect in ferroelectric, ferroelastic, or incommensurate phase transitions has become important due to the experimental availability of the so called high-accuracy universal polarimeter (HAUP) (see for example [2–5] and references therein). However, only rather occasional data exist

about materials that show pure GPTs and probably this is the reason why this type of phase transition has not yet been systematically analysed. In this way some results exist from group theoretical analysis for equitranslational GPTs associated with a single irreducible or physically irreducible representation from non-gyrotropic to gyrotropic phases [6, 7] and from domain switching considerations [8]. The analysis of these non-ferroelectric and non-ferroelastic phase transitions show that the tensor covariants transforming according to the OP symmetry are compatible with two or more forms of ferroicity [9], for example, piezoelectric and gyrotropic coefficients. This means that the domain switching can be produced at least by the lowest combination of external fields that couple linearly with the OP. For this reason the GPTs where the gyrotropic domain switching is produced by the coupling of also spontaneous piezoelectric coefficients are classified as ferroelastoelectric ones in the general class of secondary ferroics [8–11].

As mentioned before, only a few experimental studies of pure GPTs can be found. To the best of our knowledge reports about only two compounds that exhibit phase transitions of this type have been made, one occurring in  $\text{CsCuCl}_3$  [12] and the other in  $(\text{C}_5\text{H}_{11}\text{NH}_3)_2\text{ZnCl}_4$  [11]. However, although in both cases we have a pure gyrotropic character, the phase transition for  $\text{CsCuCl}_3$  is of an improper type whereas we have a proper phase transition in the Zn compound. In the latter case the experimental results have revealed the existence of a ferroelastoelectric phase transition at 249 K, where the gyrotropic tensor is the lowest-rank tensor characterizing the ferroic phase. As far as we know, this is the unique case of a pure and proper GPT ( $mmm-222$ ), which is therefore well described in the framework of the Landau theory [11]. Within this symmetry class, other candidates, as  $\text{RbBeF}_3$  and  $\text{MgClBr}$ , have been proposed for experimental studies [6, 8].

The  $(\text{C}_2\text{H}_5\text{NH}_3)_2\text{ZnX}_4$  crystal, subject of this report, belongs to a general  $(\text{C}_n\text{H}_{2n+1}\text{NH}_3)_2\text{MX}_4$  family ( $\text{C}_n\text{MX}$  for short) where  $\text{C}_5\text{ZnCl}$  takes a special position, because only the compounds with  $n \geq 5$  show conformational phase transitions. Up to now, nothing had been established about the relationship between the chain length and the occurrence of the low-temperature ferroelastoelectric phase. On the other hand, the crystals with  $n = 1, 3$  and  $4$  have the same prototype high-temperature phase as  $\text{C}_5\text{ZnCl}$  but they exhibit a ferroelastic non-gyrotropic low-temperature phase [13–15]. Therefore, the study of  $\text{C}_2\text{ZnCl}$  is interesting in order to complete a systematic experimental study of the possible influence of the organic chain length in the SPT sequences in the  $\text{C}_n\text{ZnCl}$  family.

The aim of this paper is to report structural, optical and calorimetric measurements on  $\text{C}_2\text{ZnCl}$  crystals in order to complete a systematic experimental study of the structural phase transition sequences present in the  $\text{C}_n\text{ZnCl}$  family with  $n \leq 5$ . With this study we want to establish whether the existence of a ferroelastoelectric phase is a specific property of  $\text{C}_5\text{ZnCl}$  and therefore to analyse whether the presence of the optical activity in this compound can be related to the flexibility of the organic chain. Also we want to establish an experimental framework for future microscopic approaches and complementary spectroscopic experiments.

## 2. Experimental details

The crystals were grown by means of a controlled slow-evaporation method from suprapure quality starting products. Chemical analysis give the following results (theoretical values in brackets): Cl = 46.95% (47.37), C = 15.95% (16.05), N = 9.48% (9.36), H = 5.32% (5.39), and Zn = 21.54% (21.84).

Infrared spectra between 400 and  $4000\text{ cm}^{-1}$  show no evidence of crystallization solvent in the crystals. The heat capacity measurements were made using an adiabatic calorimeter [16]. The  $C_p$  accuracy is better than 0.1% and the temperature control better than 1 mK. The calorimeter vessel was filled with about 30 g of a powdered sample with an He atmosphere of 10 Torr. The experimental set-up allows for two measuring methods: a discontinuous heating procedure and thermogram techniques. Optical measurements were made in the 15–300 K temperature interval by means of the classical rotating analyser method and an automatic Senarmont method, which allows a direct recording of the optical path against temperature [11, 17]. Complementary orthoscopic and conosopic observations were made by means of a polarization microscope with a cooling set-up. A preliminary structural analysis was performed using single-crystal x-ray diffraction techniques. Lattice constants and the space group at room temperature were determined from x-ray diffraction patterns obtained with a precession camera. Next, in order to study the structural transformations as a function of temperature a crystal was mounted in a four-circle diffractometer with a low-temperature device. The temperature stability was better than 1 K.

### 3. Results

Figure 1 shows the specific heat curve in the 70–360 K temperature interval. A specific heat anomaly with a very strong temperature dependence is evident at  $234.3 \pm 0.05$  K. The experimental points were obtained by the discontinuous heating method far from the specific heat anomaly (135 points), and three independent thermograms (continuous heating technique) were made near  $T_c$ . This latter procedure allows us to define more accurately the shape of the anomalous specific heat curve. The thermal relaxation times show a normal behaviour, but there is a small temperature range, just below the transition temperature, where the equilibrium times were exceptionally high (up to 3 h).

The thermodynamic function values for this phase transition have been determined with the help of a theoretical specific heat baseline, which takes into account both the harmonic and anharmonic contributions of the crystal lattice to the specific heat. In a previous work [15], we calculated the specific heat contribution of each methylene group in the Zn family. We also showed that this contribution is practically independent of the number of C atoms in the organic chains, in agreement with similar results obtained for other layer compounds [18]. These facts, together with the available spectroscopic information [15], permitted us to generate suitable specific heat baselines for the various Zn crystals in the medium-temperature range. The baseline obtained together with the experimental points, are shown in figure 1. Subtracting the two quantities and using a numerical integration we obtained the following values for the phase transition thermodynamic functions:  $\Delta H/R = 410 \pm 20$  K and  $\Delta S/R = 1.8 \pm 0.1$ .

Figure 2 shows the optical path measurements along the  $[0, 0, 1]$  direction in the temperature range 15–330 K. The discontinuous change at 234 K and the thermal hysteresis observed ( $\Delta T = 7$  K) confirmed the first-order character suggested by the shape of the specific heat peak. The thermal hysteresis was also confirmed by differential scanning calorimetry (DSC) measurements and its value is consistent with the analysis carried out for a similar phase transition in  $C_5ZnCl$  crystal from the point of view of Landau phenomenology [11]. In the same figure, it can be observed that the optical path goes through zero at 25 K. This fact confirms the existence of an isotropic point, which seems to be a common characteristic of this group of layer compound. The experimental values of the optical path

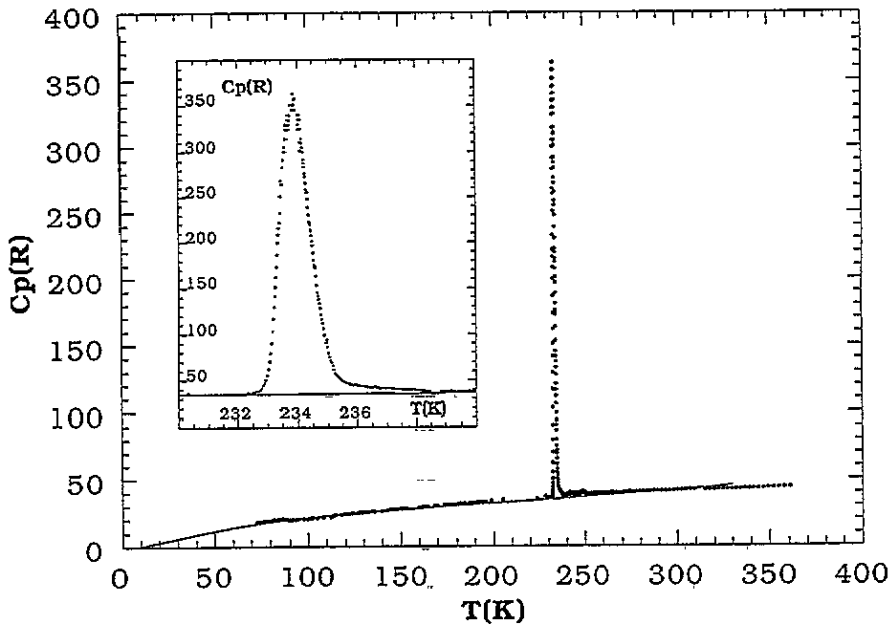


Figure 1. The specific heat of  $C_2ZnCl$  in the temperature range 70–350 K measured by adiabatic calorimetry. The inset shows the specific heat around the orthorhombic–monoclinic phase transition at 234.3 K. A short tail above  $T_c$  can be observed.

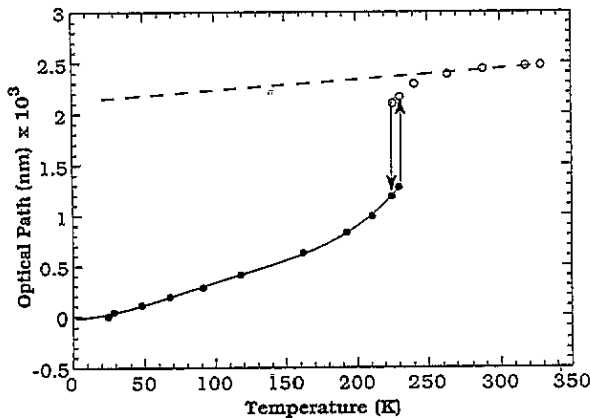


Figure 2. The optical path in  $C_2ZnCl$  against temperature. The thermal hysteresis ( $\sim 7$  K) of the first-order phase transition and the zero value (isotropic point) attained at 25 K are easily observable. The continuous line shows the fit obtained from equation (5). The dashed line is the non-spontaneous contribution to the linear birefringence.

above the phase transition (birefringence) show a very small linear temperature dependence except near 234 K, where a gradual decrease occurs. This behaviour is in agreement with the tail that the specific heat curve shows in the same temperature region. An analysis of

this behaviour is carried out in section 4.

X-ray measurements shown that the room-temperature phase is orthorhombic with lattice parameters  $a = 9.99(1)$  Å,  $b = 7.379(3)$  Å, and  $c = 17.55(2)$  Å at 295 K. The systematic absences,  $h + 1 = 2n + 1$  for  $[0kl]$  and  $h = 2n + 1$  for  $[hk0]$ , point to the  $Pnma$  space group if a centre of symmetry is assumed. As expected, this space group is the same in the high-temperature phase of the remaining short-chain  $C_nZnCl$  compounds for  $n \leq 5$ . In the low-temperature phase only the systematic absences  $h = 2n + 1$  for  $[h00]$ ,  $k = 2n + 1$  for  $[0k0]$  and  $l = 2n + 1$  for  $[00l]$  are observed, and the lattice parameters at 150 K are  $a = 7.603(4)$  Å and  $c = 16.894(7)$  Å with interaxial angles of  $90^\circ$  within their standard deviation ( $\sigma < 0.05^\circ$ ). The experimental results allow us to assume the  $P2_12_12_1$  as the low-temperature space group, even if intensity equivalence of orthorhombic symmetry related reflections were not fully observed for all reflections treated. This effect is explained by the anisotropic form of the crystal and its absorption coefficient ( $\mu = 99$  cm $^{-1}$  for Cu K radiation).

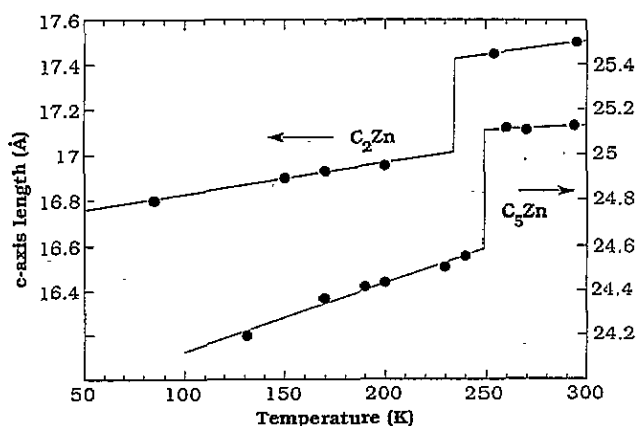


Figure 3. The  $c$ -axis length of  $C_2ZnCl$  and  $C_5ZnCl$  from 100 K to 300 K. A similar thermal expansion step per C atom in the two crystals should be noted.

Figure 3 shows the temperature dependence of the  $c$ -axis length between 100 K and 300 K for both  $C_2ZnCl$  and  $C_5ZnCl$  crystals. The step value of the discontinuous change in both compounds is proportional to the chain length. These results are in agreement with previous thermal expansion measurements [11], as well as with the first-order character of this phase transition.

#### 4. Discussion

The experimental results in this paper together with those in [11] show that  $C_2ZnCl$  and  $C_5ZnCl$  undergo similar ferroelastoelectric low-temperature phase transitions. These crystals show the same  $Pnma$ - $P2_12_12_1$  phase transition sequence, and the temperature dependence of the specific heat, optical path, and thermal expansion ( $c$ -axis values) (figures 1–3) are

also similar in the two compounds. Orthoscopic observation with white light shows an incomplete extinction below 234 K, while the extinction is complete at room temperature where the optical activity is forbidden by symmetry. This fact is also experimental evidence of an anomalous optical dispersion with a significant wavelength dependence of the linear birefringence.

The group theoretical analysis for this equitranslational phase transition ( $Pnma \rightarrow P2_12_12_1$ ) reveals that the irreducible representation according to which the order parameter transforms is  $A_u$ . This means that only the magnitudes transforming according to  $A_u$  will be spontaneous in the distorted phase. Three piezoelectric and three gyrotropic tensor components have  $A_u$  symmetry. This means that each component or a linear combination of them could be the OP of this phase transition. Within this picture  $C_2ZnCl$  can be considered as a secondary ferroic with a ferroelastoelectric low-temperature phase. The appearance of the crystal under the polarizing microscope confirms the group theoretical analysis in complete agreement with the results for the  $C_5ZnCl$  crystal [11]. The conoscopic pattern and the domain structure are the same in the two crystals.

From a structural point of view, the compounds  $C_2ZnCl$  and  $C_5ZnCl$  have some common characteristics. In the parent phase the position of the alkylammonium chains is either restricted to a mirror plane or disordered between two symmetric positions related by this plane. Furthermore all the chains are essentially parallel to the normal of the inorganic layer. As regards the low-temperature phase in  $C_5ZnCl$ , the mirror plane is no longer present and the chains are homogeneously tilted with respect to the normal of the  $ZnCl_4$  layer in order to form a close packing. In this crystal, the organic chains in the low-temperature phase are nearly in all *trans* configuration with a bending angle of about  $14^\circ$ . The bending of the chains shortens the inorganic interlayer distances (*c*-axis) by a factor of 2.3%. This is just the value also obtained for  $C_2ZnCl$  from x-ray measurements. This fact is in complete agreement with the experimental measurements shown in figure 3, where we observe that the thermal expansion step per C atom is the same in the two compounds.

In addition, the specific heat peak value, the transition temperature, and the transition entropy found for  $C_2ZnCl$  are very close to those in  $C_5ZnCl$  ( $T_c = 249.65 \pm 0.05$  K,  $\Delta S/R = 1.73 \pm 0.2$ ). This result, together with the analysis of the thermal expansion step, seems to confirm that the microscopic mechanism of this particular transition should be exclusively related to the freezing of the dynamical disorder of the N-H...Cl hydrogen bond, which links the organic chain to the inorganic layer. This fact is considered to be responsible for the observed chain tilting, rather than order-disorder effects in the alkyl chains, which are otherwise present only in the higher-temperature phases of  $C_5ZnCl$ .

According to the experimental results in this paper the distorted phase exhibits simultaneously birefringence and optical activity. In our case the optical measurements combine the two effects and can be analysed using a principle of superposition [1]. In general the optical activity is a weak effect as compared with the birefringence and is easily overwhelmed by it. However, as we see later, the experimental curve must be compatible with the theoretical predictions of both birefringence and optical activity through their dependence on the order parameter. The superposition principle shows that there are two elliptically polarized modes of propagation with a phase retardation given by

$$\Omega(T) = (2\pi d/\lambda_0) \left[ (\Delta n)^2 + (G/\bar{n})^2 \right]^{1/2} \quad (1)$$

where  $d$  is the crystal thickness,  $\Delta n$  is the birefringence,  $\lambda_0$  is the free space wavelength,  $\bar{n}$  is the mean refractive index for the two modes, and  $G$  is the gyration for a particular

direction given by  $G = \pm \sum_{i,j} g_{ij} l_i l_j$ , where  $g_{ij}$  are the tensor components and  $l_i, l_j$  are the direction cosines relative to the chosen axes. In our case  $G = \pm g_{33}$ , and  $\Omega(T)$  is given through the temperature dependence of  $\Delta n$  and  $G$ .

In the framework of the Landau theory and assuming a first-order character for the phase transition [11], the temperature dependence of the OP ( $\eta(T)$ ) is given by

$$\eta^2 = \frac{2}{3}\eta^2(T_c) \left[ 1 + \left[ 1 - \frac{3}{4}(T - T_0)/(T_c - T) \right]^{1/2} \right] \quad (2)$$

where  $T_c$  is the transition temperature and  $T_0$  the limit of stability of the high-temperature phase. From the group theory analysis all the modes with  $A_u$  symmetry are proportional to  $\eta(T)$  and those with  $A_{1g}$  symmetry couple quadratically with the order parameter and therefore are proportional to  $\eta^2(T)$ . In our case the temperature dependence of both the spontaneous birefringence ( $\Delta n_s$ ) and the gyration coefficient ( $g_{33}$ ) in the distorted phase can be written by the following proportionality relations:

$$\Delta n_s \alpha \eta^2(T) \quad g_{33} \alpha \eta(T). \quad (3)$$

In our case the crystal is birefringent in the prototype phase and therefore the birefringence in the distorted phase is given by

$$\Delta n = \Delta n_p + \Delta n_s \quad (4)$$

where  $\Delta n_p$  is the non-spontaneous contribution to the linear birefringence (nearly constant in both distorted and prototype phases) and  $\Delta n_s$  is the spontaneous linear birefringence in the ferroelastoelectric phase. Equations (3) and (4) in (1) allow us to write the optical path as follows:

$$\Omega(T) = (2\pi d/\lambda_0) [A + B\eta^2(T) + C\eta^4(T)]^{1/2} \quad (5)$$

where  $A$  is related to  $\Delta n_p$ , and  $B$  and  $C$  are constants related to the coefficients of the usual Landau free expansion for first-order phase transitions and with the proportionality factors in (3). The fit of the experimental points to equation (4) using the temperature dependence of the OP given by (2), is shown in figure 2, and is similar to those found for  $C_5ZnCl$ . However, additional experimental information using the HAUP technique would be desirable in order to obtain quantitative values of  $\Delta n_s$  and  $g_{33}$  and to calculate quantitative Landau coefficients.

The Landau predictions can be compared with other physical quantities. So, for instance, according to the Landau approach the anomalous part of the specific heat should satisfy the equation

$$\Delta C_p \alpha \begin{cases} T(T_d - T)^{1/2} & T < T_c \\ 0 & T > T_c. \end{cases} \quad (6)$$



However, although these equations successfully describe the specific heat behaviour for a great number of first-order phase transitions, the experimental points in figure 1 show, within  $\pm 1$  K around the transition temperature, a much stronger temperature dependence than equation (6). The same specific heat behaviour is exhibited by  $C_3ZnCl$  near  $T_c$ , and by other compounds with first-order structural phase transitions [19–21]. The measured curves show a good agreement with the Landau theory except close to  $T_c$ , where a strong specific heat divergence cannot be described by equation (6), even if higher-order terms are included in the free energy expansion. Above room temperature the specific heat curve and optical path measurements show a short tail and a gradual decrease starting just above the transition temperature. It must be taken into account that in agreement with (2) the gradual decrease in the optical path leads to a short tail in the order parameter above  $T_c$ . The deviations from the classical behaviour above  $T_c$  are commonly attributed to defects and crystal inhomogeneities [19–22], which explain the tails in both specific heat and order parameter (optical path). However, in our case, the specific heat curve and the optical path behaviour are the response of two microscopic mechanisms: order–disorder and displacive. The two mechanisms could have a different temperature dependence, which could explain the deviations from the Landau behaviour near  $T_c$ . In both crystals, a good fit of the specific heat experimental points near  $T_c$  has been attained by the addition of an asymmetric power law term to equations (6). ( $C_p \propto |T - T_c|^\alpha$  for  $T < T_c$  and  $C_p \propto |T - T_c|^{\alpha'}$  for  $T > T_c$ ). However, in this case the  $\alpha$  and  $\alpha'$  exponents are not relevant to explaining this behaviour within the critical exponent theories, because the values obtained are very much higher than the theoretical predictions.

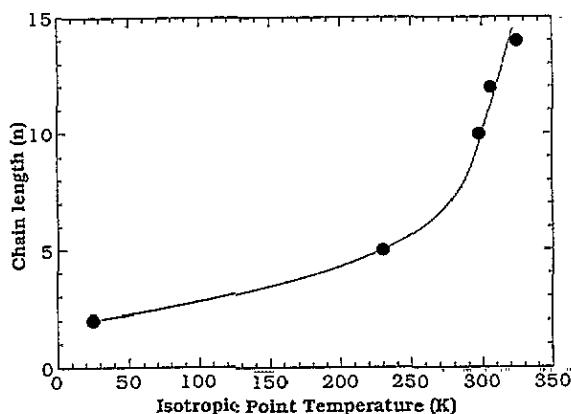


Figure 4. The isotropic point temperatures for the  $C_nZnCl$  family. The temperature shows an asymptotic behaviour for larger  $n$  values and a strong dependence on  $n$  for  $n \leq 5$ .

As mentioned before,  $C_2ZnCl$  shows an isotropic point around 25 K. In this point the crystal goes from a biaxial conoscopic pattern to one  $90^\circ$  rotated through an intermediate uniaxial pattern. This optical anomaly is present as well in other members of this family of compounds with different cations and chain lengths [11, 23, 24]. Figure 4 shows for the  $C_nZnCl$  family the  $n$  dependence of the isotropic point temperature. As can be seen in this figure the isotropic point shows a strong dependence of temperature on  $n$  for  $n \leq 5$  and an asymptotical behaviour for larger  $n$  values. As the isotropic point temperature is also

wavelength dependent [23, 24], this family of compounds can be considered as a source of promising candidates for temperature calibrations in spectroscopic systems. In any case, the systematic study of this anomaly in transparent and absorbent members of this family in order to elucidate the microscopic mechanisms is an open problem at the moment.

## 5. Conclusion

The experimental results in this paper open up new possibilities for  $C_nMX$  materials in connection with the GPTs as well as with optical dispersion measurements. In any case quantitative measurements of gyrotropic coefficients will be interesting in order to confirm the existence of deviations of the Landau predictions near  $T_c$  as well as to look for microscopic approaches. Finally it is worth while noticing that an interesting question related to the microscopic aspects of the optical activity remains open: why among five compounds of the same family ( $1 \leq n \leq 5$ ) with the same prototype phase and similar microscopic mechanisms in the low-temperature phase transition [11, 13, 14] do only two of them ( $n = 2$  and 5) show a low-temperature gyrotropic phase?

## Acknowledgments

This work was supported by the following projects: UPV/EHU-063.310-TO 13/91 and 063-310-EB109/92 of the Universidad del Pais Vasco, DGICYT-PB91-554 of the Spanish Government, and No 63.310.0012/91 of the Basque Government.

## References

- [1] Nye J F 1957 *Physical Properties of Crystals* (Oxford: Clarendon)
- [2] Kobayashi J and Uesu Y 1983 *J. Appl. Crystallogr.* **16** 204
- [3] Uesu Y and Kobayashi J 1985 *Ferroelectrics* **64** 115
- [4] Saito K, Sugiyama H and Kobayashi J 1990 *J. Appl. Phys.* **68** 732
- [5] Ortega J, Etxebarria J, Zubillaga J, Breczewski T and Tello M 1992 *Phys. Rev. B* **45** 5155
- [6] Konac C, Kopsky V and Smutny F 1978 *J. Phys. C: Solid State Phys.* **11** 2493
- [7] Aizu K 1973 *J. Phys. Soc. Japan* **34** 121
- [8] Cross L E and Newnham R E 1977 *Ferroic Crystals for Electro-optic and Acousto-optic Applications* (Philadelphia, PA: Pennsylvania University) appendices VII and VIII
- [9] Wadhawan V K 1970 *Acta Crystallogr.* **35** 629
- [10] Wadhawan V K 1982 *Phase Transitions* **3** 3
- [11] Gómez-Cuevas A, Pérez-Mato J M, Tello M J, Madariaga G, Fernández J, López-Echarri A, Zúñiga F J and Chapuis G 1984 *Phys. Rev. B* **29** 2655
- [12] Hirotsu 1975 *J. Phys. C: Solid State Phys.* **8** L12
- [13] Pérez-Mato J M, Mañes J L, Fernández J, Zúñiga F J, Tello M J, Socías C and Arriandiaga M A 1981 *Phys. Status Solidi a* **68** 29
- [14] Zúñiga F J, Tello M J, Pérez-Mato J M, Pérez-Jubindo M A and Chapuis G 1982 *J. Chem. Phys.* **76** 2610
- [15] López-Echarri A, Zubillaga J and Tello M J 1988 *Solid State Commun.* **68** 185
- [16] López-Echarri A and Tello M J 1981 *J. Phys. D: Appl. Phys.* **14** 71
- [17] Wood I G and Glazer A M 1980 *J. Appl. Crystallogr.* **13** 217
- [18] White M A 1984 *J. Chem. Phys.* **81** 6100
- [19] Stokka S and Fossheim K 1982 *J. Phys. C: Solid State Phys.* **15** 1161
- [20] Stokka S, Fossheim K, Johansen T and Feder J 1982 *J. Phys. C: Solid State Phys.* **15** 3053

- [21] Stokka S and Fossheim K 1981 *Phys. Rev. B* **24** 2807
- [22] Aharony A and Hohenberg P C 1976 *Phys. Rev. B* **13** 3081
- [23] Arriandiaga M A, Socías C, Fernández J, Gómez-Cuevas A, Tello M J, Herreros J and López-Echarri A 1984 *Solid State Commun.* **51** 477
- [24] Fernández J, Gómez-Cuevas A, Arriandiaga M A, Socías C and Tello M J 1985 *Phys. Rev. B* **31** 4562